International Journal for Housing Science and Its Applications
Publish August 4, 2025. Volume 46, Issue 3 Pages 2460-2472

https://doi.org/10.70517/ijhsa463205

Experimental study and simulation analysis of freezing expansion of a single geocell

Feng Wang[1], Ling Song[1,*] and Jie Liu[2]
[1] College of Water Conservancy & Architectural Engineering, Shihezi University, Shihezi, Xinjiang, 832003, China
[2] Science and Technology R&D Center, Xinjiang Transport Planning Survey and Design Institute Co. Ltd., Urumqi, Xinjiang, 830000, China
Corresponding authors: (e-mail: 15516560897@163.com).

Abstract Geocell-reinforced soil has been widely applied in engineering projects in permafrost regions, but its mechanical behavior during the frost heaving process still requires in-depth research. This article conducts low-temperature frost heave tests to evaluate individual geocell-reinforced soil samples with varying water contents. Based on the experiments, a three-dimensional numerical model is established to simulate the interaction between the soil and the geocell, and to analyze the variation patterns of temperature, moisture, displacement, and frost heave strain. Then, the reinforcement effects of geocells with different shapes are compared. The results indicate that the geocell exhibits significant non-uniform strain distribution during the frost heave process. Moreover, the higher the water content, the greater the frost heave displacement. By comparing geocells of different shapes, it was found that circular geocells perform best in restricting soil frost heave. The application of geocells in frozen soil regions can enhance the frost heave performance of soil, and this study provides a theoretical basis for geocell-reinforced engineering in such areas.

Index Terms Geocell, Frost heave test, Geocell shape, Finite element method

I. Introduction

With the development of technology and the expansion of application, geocell reinforced soil has been widely used in highway, railroad, water conservancy and other projects. A large number of on-site, indoor and simulation tests have shown that geocells can effectively enhance the mechanical properties of weak soils, improve the bearing capacity of soils, and also control the post-work settlement and uneven settlement of foundations, which is outstanding in improving structural stability and durability. In the engineering practice of permafrost zone, it is often necessary to take some measures to mitigate freeze-thaw damage. The separation, reinforcement, drainage and filtration functions of geocell materials, as well as the friction, locking and impedance effects on the reinforced soil body, make geocell reinforced soil often used as a treatment measure to mitigate permafrost geological hazards.

Geocell reinforced soil in permafrost roads, embankments and other engineering applications to improve the structural stability and durability of the project has been verified. Liu Jianqi [1] and Wang Zhenduo [2] introduced the construction technology of geocells for reinforcing roadbeds in permafrost areas and for channel shoring, aiming at solving the problem of permafrost frost damage. Wei Jing [3] tested the deformation of geocells used for geocell slope protection on roadbed slopes in perennial permafrost areas, and the results showed that geocells used for roadbed slope protection in perennial permafrost areas were feasible and gave engineering treatment measures. Wang Tiequan [4], Wang Liyun [5], Mao Xuesong [6], etc. Combined with the Tibetan Plateau permafrost region of geocell reinforcement and other pavement structures for disease monitoring, research and analysis found that the geocell reinforced pavement resistance to cracking ability is better than other grass-roots pavements.

In addition, foreign researchers DEHGHANİAN [7] gave an overview of the freeze-thaw behavior of geocell reinforced foundations and concluded that geocells improve road durability by draining water and forming capillary barriers during spring thawing and thawing.Pokharel et al [8]-[10] carried out a long period of continuous monitoring on geocell reinforced roads in Alberta, and verified that by measuring the depth of rutting and other experimental methods The service performance of the reinforced pavement after freeze-thaw.Huang et al [11]-[13] developed a geocell freeze-thaw model experimental setup to investigate the effect of mechanical behavior of geocell reinforced and unreinforced soil in freeze-thaw tests and concluded that geocells can improve the mechanical properties of sandy soils by 30-110% after conducting unit and multiple geocell freeze-thaw cycles as well as flat plate loading tests.

It can be seen that although geocells have been widely studied and applied, the limiting effect of geocells on the freezing process through the formation of three-dimensional lattice structures in permafrost regions still needs to be

further explored. Therefore, this paper investigates the effect of soil reinforcement under the flexible lateral limit of geocells, introduces a single geocell freezing model on the basis of experiments, and further explores the effect of different shapes of grid cells on the reinforced frozen soil.

II. Freeze-up test of single geocell reinforced soil

II. A. Test materials

Based on the field engineering to take test soil samples, soil samples according to the “Geotechnical Test Procedures” to get the particle grading curve shown in Figure 1, the soil samples inhomogeneity coefficient of about 15.5, greater than 5; coefficient of curvature of about 1.67, between 1 ~ 3, the soil particles particle size distribution is uniform and well-graded. The basic physical properties of the soil body are shown in Table 1.

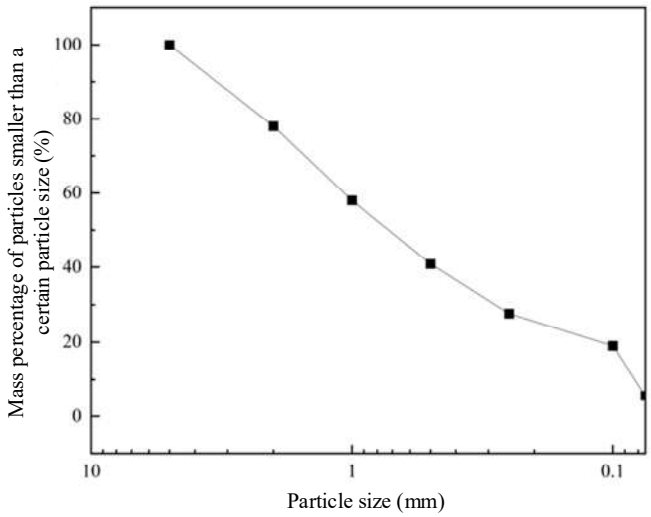

Figure 1: Particle grading curve

Table 1: Physical properties of soil

Class	Proportion Gs	Poisson ratio	Internal friction angle / (°)	Cohesive strength / (kpa)
Sandy loam	2.69	0.291	25	28

The high-strength geocells used in the test for high-density polyethylene ultrasonic welding geocells, geocells, geocells, geocells and other technical requirements to meet the specific requirements of JT / T 516-2004 “highway engineering geosynthetics geocells, geocells, geocells, geocells, geocells, geocells, geocells, geocells, geocells, geocells, geocells and geocells, geocells and geosynthetics. Height is 20 cm.

II. B. Test equipment and test procedure

The test process mainly includes the following steps: mixing soil samples with different moisture contents, pasting sensors, and filling and compacting sandy soil. Before the experiment, the soil samples with different water contents were configured. As the test for different water content of a single geocell structure for frost expansion test, so before the test need to take a certain amount of soil samples, and then take the corresponding amount of water to configure the soil samples into the water content of 10%, 15%, 20%. Before the configuration of the corresponding water content of the soil sample, take about 25 kg of soil samples, through the drying oven to dry the soil sample water, soil samples need to add the mass of water according to the following formula:

$$m_w = \frac{m_s}{(1+w_0)} \times (1+w_1) - m_s \tag{1}$$

In the above equation, m_w is the mass of soil required to add water, m_s is the mass of soil, w_0 is the initial water content, and w_1 is the final water content of the soil sample. For controlling the initial compaction of the specimen, the required added soil mass m is calculated as:

$$m = K \cdot \rho_{d\max} \cdot V(1+w) \tag{2}$$

In the above equation: K is the initial compaction (%) set for the soil sample; $\rho_{d\max}$ is the maximum dry density of the prepared soil sample, which takes the value of 1.69 $g \cdot \mathrm{cm}^{-3}$; V is the volume of soil loaded in the specimen (cm^3), which takes the value of 1.4×104 cm^3; w is the moisture content (%) of the soil material to be compacted.

Since the soil samples were dried in a drying oven, the initial water content of the soil samples w_0 =0. The dried soil samples were weighed and the mass of water to be added was calculated, and the soil samples were mixed by a SJD-15 small mixer. Add the soil sample and the required mass of water to the mixer and mix thoroughly for 120 s. After mixing, pour out the mixer and test the homogeneity of the soil sample and put it in a plastic bag for the test.

Before the start of the test, mark 20 mm, 100 mm and 180 mm inside the wall of the geocell, then place the geocell in the middle of the base of the bearing box, spread the plastic film at the bottom and around the geocell, pour the soil samples mixed with water into the geocell, the geocell is fully expanded when filling, and the soil material is filled in layers, scraped flat and compacted. In the process of pasting sensors, the sensors were numbered and marked, and then the thermocouples and strain gauges were fixed in the wall of the geocell with glue, in which the thermocouples T1, T2 and T3 were pasted in the upper, middle and lower parts of the wall of the geocell for a total of 3, while the strain gauges #1, #2 and #3 were pasted in the upper, middle and lower parts of the center line in the wall of the chamber, and the strain gauges #4, #5 and #6 were pasted in the welded seams in the wall in the upper, middle and lower parts, for a total of 6. The strain gauges #4, #5 and #6 are pasted at the upper middle and lower position of the weld seam inside the wall, total 6, the pasting position is shown in Fig. 2(b), the sensors are wrapped with the waterproof tape after pasting and the data line, which can isolate the effect of moisture on the sensors on one hand, and prevent the sensors from destruction during filling and compaction of the soil on the other hand. The distance between the welded seams of the geocells after compaction was measured to be 36.0 cm, and the distance between the center of the cell walls was 26.5 cm.

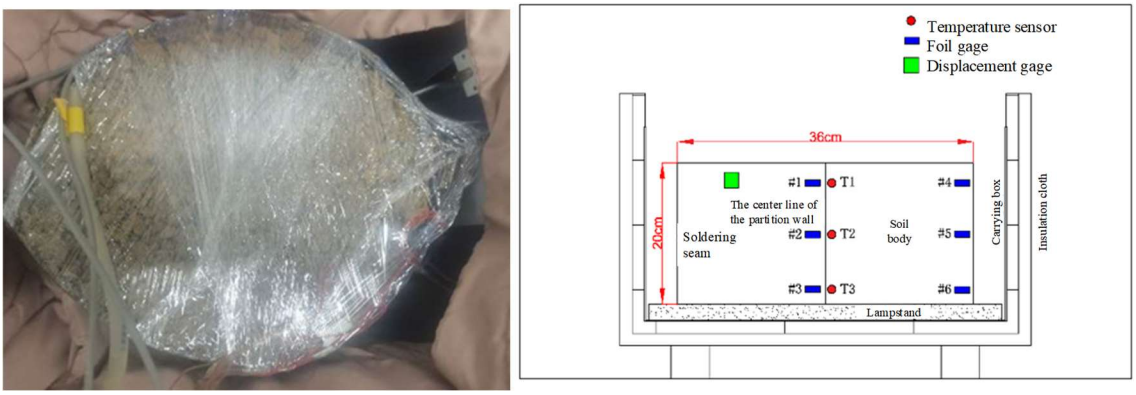

(a) Single geocell specimen (b) Schematic diagram of monitoring point layout

Figure 2: Single geocell sample layout

To prevent moisture loss, all geocell specimens were sealed with plastic film throughout the freezing process. Insulation measures were applied to the bottom and sides of the load box containing the geocells to realize top-down freezing of the soil inside the cryostat. To ensure uniform temperature distribution in the soil samples, the ambient temperature was set at 1°C for 24 h. During the freezing process, the test chamber was set at -2°C for 120 h. At this time, the coolant circulating in the chamber cooled the geocell-filler structure, and the top-down freezing of the soil inside the chamber was realized by utilizing the insulating cloth to isolate the cold air. At the same time, in order to facilitate the measurement of the change of water content after freezing at different locations of the geocell, through the freezing of soil columns without geocell side limit isometrics, and then take out and measure the total moisture content at different heights after the completion of the measurement.

III. Modeling of freezing expansion of individual geocells

In order to compare and verify with the experimental results, COMSOL finite element numerical simulation was carried out in the paper to study the frost expansion of a single geocell. In the geocell reinforced soil numerical simulation, more than two-dimensional planar analysis method, in order to visually analyze the interaction characteristics and deformation of geocells and fill structures both in the perennial permafrost zone. It is assumed

that the geocell retaining wall of the uppermost single cell-fill is separated out, and the deformation of its structural body is analyzed in the freezing process under the consideration of linear elasticity only. Before numerical simulation, the following basic assumptions are made:

(1) The soil particles are incompressible and have no deformation during the freezing and thawing process, the effect of salt in the soil is ignored, and only the volume change caused by the freezing and expansion of water in the soil is considered;

(2) The effect of friction between soil and geocell is not considered, and there is no relative sliding between geocell material and soil;

(3) Only the migration of liquid water is considered, not the migration of gaseous water;

(4) Assuming that the soil body is homogeneous and isotropic, each hydraulic conductivity and thermal conductivity of permafrost are constant;

(5) Pore water seepage obeys Darcy's law;

(6) Neglect the effect of external loading on the geocell specimen.

III. A. Basic equations

When phase change occurs in water and ice, the heat of phase change is present in the soil as a heat source, so the heat transfer equation considering the heat of phase change is:

$$\rho C(\theta)\frac{\partial T}{\partial t}=\lambda(\theta)\nabla^2 T+L\cdot\rho_{\mathrm{i}}\frac{\partial\theta_{\mathrm{i}}}{\partial t} \tag{3}$$

The unfrozen water exists throughout the freezing and thawing process, selected to apply to the law of water movement in unsaturated permafrost and assumed to be similar to the thawing soil water migration law, according to the Richards equation proposed in the literature and taking into account the ice resistance in the freezing process, the equation of the moisture field is obtained as:

$$\frac{\partial\theta_u}{\partial t}+\frac{\rho_{\mathrm{i}}}{\rho_w}\frac{\partial\theta_i}{\partial t}=\nabla\left[D(\theta_u)\nabla\theta_u+k(\theta_u)\right] \tag{4}$$

The ratio of the volume content of pore ice to the volume content of unfrozen water is given by the linking equation [14]:

$$B_I=\frac{\theta_i}{\theta_u}\begin{cases}1.1\left(\dfrac{T}{T_f}\right)^B-1 & T<T_f\\ 0 & T\geq T_f\end{cases} \tag{5}$$

where the constant 1.1 is the density ratio of water to ice in the soil; B is the solid-liquid ratio coefficient, a constant that varies with soil mass and salinity, and is calculated from the literature sandy soils generally take the value of 0.61, pulverized soils take the value of 0.47, and clay soils take the value of 0.56.

The volumetric strain generated by hydrothermal coupling is used as the internal stress field of the soil to establish the stress field control equation.

Equilibrium equation:

$$-\nabla\cdot\sigma=F \tag{6}$$

Geometric equations:

$$\varepsilon=\nabla u \tag{7}$$

Ontological modeling:

$$\{\sigma\}=[D](\{\varepsilon\}-\{\varepsilon_0\}) \tag{8}$$

where: ε is the total strain; [D] is the elasticity matrix.

III. B. COMSOL-based numerical model construction

The temperature and moisture field control equations were transformed into the form of partial differential equations of the COMSOL coefficient type:

$$\begin{cases} \rho C(\theta)\dfrac{\partial T}{\partial t}+\nabla\cdot\left(-\lambda(\theta)\nabla T\right)=L\rho_i\dfrac{\partial \theta_i}{\partial t} \\ \dfrac{\partial \theta_u}{\partial t}+\nabla\left[-D(\theta_u)\nabla\theta_u-k(\theta_u)\right]+\dfrac{\rho_i}{\rho_w}\dfrac{\partial \theta_i}{\partial t}=0 \end{cases} \tag{9}$$

In this paper, the hydrodynamic freezing and expansion model [15] is used to realize the freezing and expansion of the soil body, i.e., it is considered that the soil body starts to freeze and expand when the ice content of the soil body reaches its initial freezing and expansion ice content. The distribution of ice content in the soil body is obtained from the coupled water-heat model, and then the freezing expansion of the soil body is calculated. For the assumption of freezing expansion, this paper points out that at the macroscopic level freezing expansion is an isotropic volumetric expansion, similar to the thermal expansion of other materials.

Therefore, the amount of freezing expansion of the soil body is calculated using the solid mechanics module of COMSOL, which can be expressed as:

$$\varepsilon_{th}=\alpha\left(T-T_{ref}\right) \tag{10}$$

where: ε_{th} is the strain due to thermal expansion, α is the coefficient of thermal expansion of the material, T and T_{ref} are the temperature, the instantaneous reference temperature, respectively.

The freezing expansion rate of frozen soil is expressed as:

$$\eta=\Delta h/h \tag{11}$$

where: Δh and h are the freezing height and freezing depth, respectively.

This freezing rate is the change in freezing height, or volumetric freezing rate, under lateral limit conditions. The linear freezing expansion rate can be expressed as:

$$\eta_1=\sqrt[3]{\eta+1}-1 \tag{12}$$

The coefficient of thermal expansion is replaced by the linear freezing expansion rate. In addition, the strain is disconnected from the temperature and the temperature difference $\left(T-T_{ref}\right)$ is fixed at 1. The purpose is to convert the thermal expansion module in COMSOL to a linear freezing expansion rate module, ignoring $\left(T-T_{ref}\right)$ the effect on the linear freezing expansion rate, which can be expressed as Eq:

$$\varepsilon_{inel}=\eta_1\left(T-T_{ref}\right) \tag{13}$$

$$\varepsilon_{inel}=\sqrt[3]{\eta+1}-1 \tag{14}$$

III. C. Modeling and Boundary Condition Determination

Geometric modeling

The 3D model is drawn and generated in SOLIDWORKS, and then the filler entity and geocell shell model are added through the LiveLink for SOLIDWORKS node in the COMSOL geometry, respectively, to establish the original elliptical single geocell model structure as well as the circular and square single geocell model structure. The model geometry is shown in Figure 3.

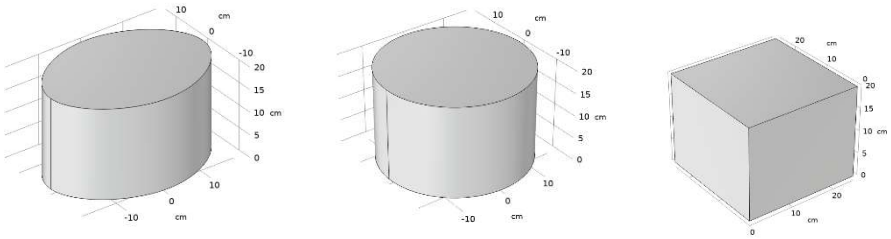

(a) oval (b) circular (c) square

Figure 3: 3D model of reinforced soil with different shape geocell

In this chapter, a temperature boundary condition is imposed in the geometric domain of the geocell structure body, so the Dirichlet condition is chosen for the thermal boundary. Due to the insulation measures applied to the bottom plate as well as the sides in the load box during the test, the numerical simulation in this chapter assumes that the geocell is adiabatic around the perimeter and at the bottom, and the heat transfer occurs only from the top [16].

In the soil simulation, the soil is regarded as macroscopically homogeneous isotropic material, and the density, initial volumetric water content, initial temperature and modulus of elasticity of the fill in the geocells are taken according to the test, and the coefficient of thermal conductivity of the soil as well as the heat capacity parameter of the soil are selected according to the recommended values of “Code for Design of Building Foundation in Permafrost Areas” (JGJ 118-2011), and the value of the parameters of the soil is shown in Table 2.

Table 2: Parameters of boundary conditions in structure during freezing test

Trial	Freeze
Soil property	Sandy loam
Altitude	20 cm
Initial moisture content	10%, 15%, 20%
Upper temperature	-2℃
Lower temperature	Adiabat
Solid-to-liquid ratio	$2.94\|T\|\quad -1.1$

The temperature effect of the reinforcement is not considered, while the maximum tensile strain produced by the lattice chamber reinforcement under ultimate load is only 5%, so the geocell material can be regarded as orthotropically isotropic and linearly elastic material in the finite element simulation. The orthotropic anisotropy parameters of geocells in the geometric model of compartment-filler [17] are shown in Table 3.

Table 3: Orthogonal anisotropy parameters of geocell

Material properties	Numeric value	Unit
$\{E_1, E_2, E_3\}$	$\{1.4, 1.4, 7.4\}$	MPa
$\{G_{12}, G_{23}, G_{13}\}$	$\{3.34, 4.16, 4.16\}$	MPa
$\{\upsilon_{12}, \upsilon_{23}, \upsilon_{13}\}$	$\{-0.065, 0.06, 0.06\}$	-

The temperature and moisture fields are established using partial differential equations in the form of coefficients in the PDE module, respectively, and the solid mechanics interface is used to solve for the stress field variations. The geocell is simulated using a shell model with linear elasticity, and COMSOL provides a multi-physics field node entity-thin structure connecting multi-physics field node, which can be used to connect the shell physics field of the geocell with the solid mechanics physics field.

IV. Analysis of test and simulation results

IV. A. Temperature field analysis

Figure 4 geocell-filler structure body in the low temperature environment at different heights undergo 120h temperature change, as can be seen from the figure, the simulation results and test results are basically the same, in the initial freezing time within 10h, geocell wall temperature from 1 ℃ began to cool down and rapidly decline, this is due to the structure body at the top position of the temperature gradient is larger, this time has not yet occurred in the ice-water phase transition, no ice crystals appear, and the temperature After reaching the freezing temperature, the free water in the soil body undergoes a phase transition and freezes rapidly, forming ice crystal nuclei that grow rapidly; between 10 and 60h of freezing time, the temperature starts to become slow, and this process results in a slower temperature drop due to the heat absorption of the water phase into ice; after 60h, the temperature is basically unchanged.

In addition, during the cooling process of the test chamber, the sensor T1 of the contact surface close to the ambient temperature decreases faster, and the rate of change of the temperature gradually becomes smaller with the increase of the burial depth. This is because in the freezing process, the geocell as a whole is cooled in a top-down manner, and the temperature is hindered by the water ice in the soil body during the infiltration change. Therefore, the closer the soil body within the geocell is to the surface temperature change of the upper soil will be lower, and fall faster, thus forming a temperature gradient from the surface of the structure to the deeper layers of the incremental change.

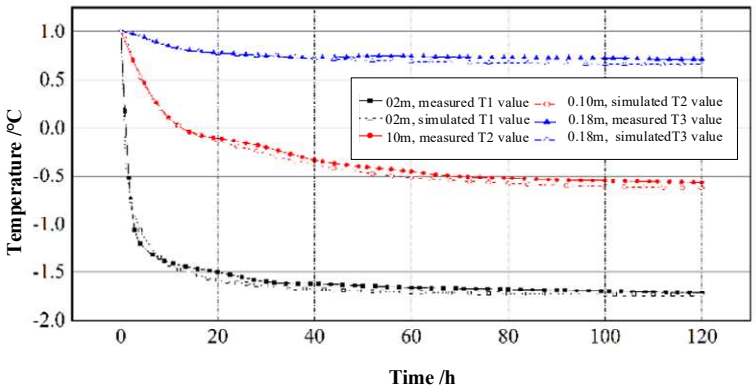

Figure 4: Temperature-time relationship of soil at different depths

Figure 5 shows the simulated cloud maps of the temperature field in the cut surface of the structure body at different times. With the increase of cooling time, the freezing front gradually passes downward, and at 10h of freezing, the freezing front starts to appear at 5.6cm from the top of the structure body, and the temperature change slows down from 40h, and the freezing front remains constant at 9.1cm from the top.

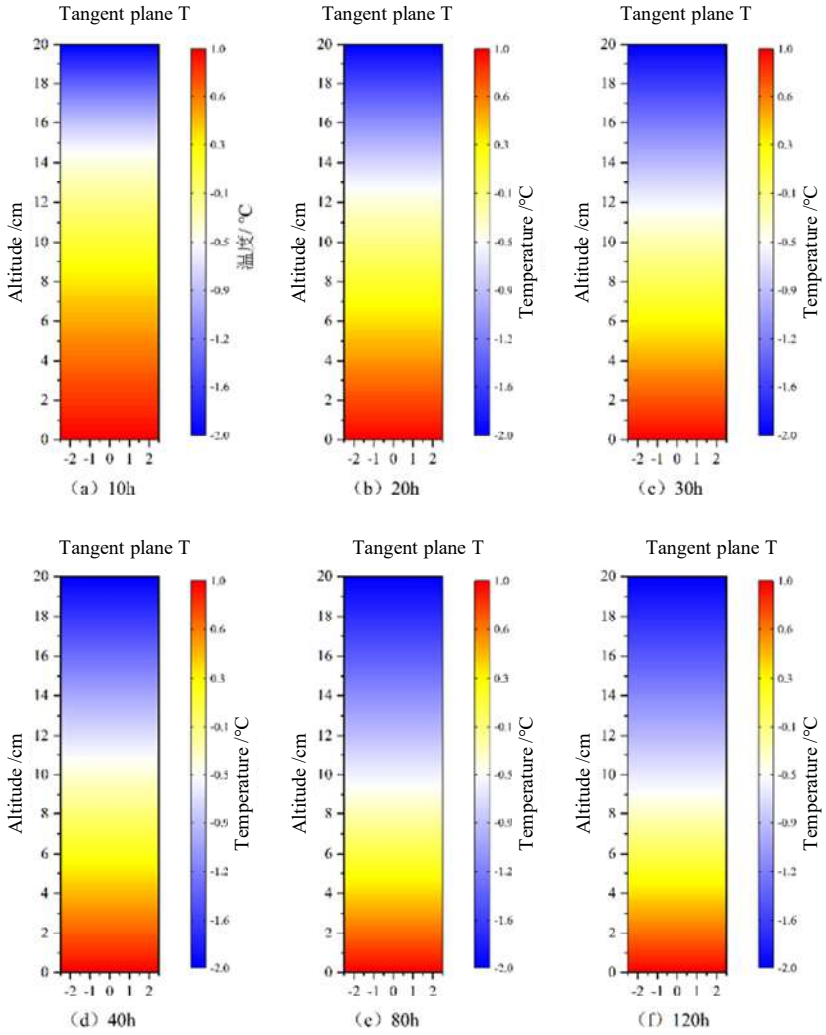

Figure 5: Temperature field simulation cloud map

Figure 6 shows the distribution of temperature along the height of the structure at different freezing times, from the figure, it can be seen that from the room temperature of 1 ℃, the first 10h temperature change gradient is the largest and the temperature difference between the top and the bottom of the structure body is obvious, this is because the temperature in the structure body drops to the freezing temperature, the liquid water in the permafrost at the temperature of the phase change, at the same time, the formation of the temperature is transmitted from top to bottom in the temperature incremental gradient change in the 10 ~ 40h change The amplitude slows down, and after freezing for 40h, there is no obvious difference in the temperature change gradient at the bottom end of the reach until the freezing front of the structure body is not changing.

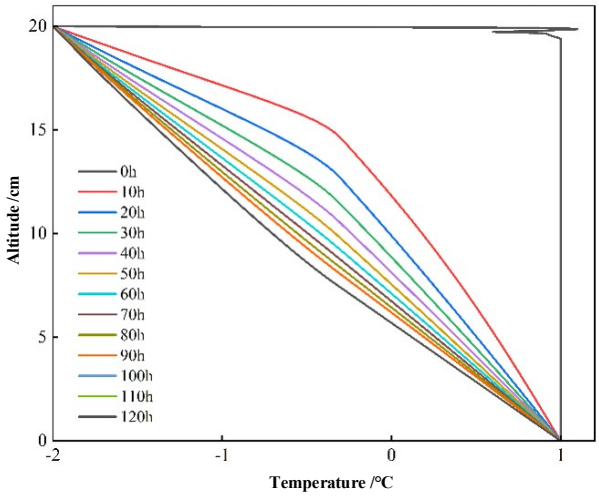

Figure 6: Temperature distribution along the height of the structure at different times

IV. B. Hydraulic field analysis

Figure 7(a) shows the schematic diagram of the contour soil column under the side limit after freezing, from which it can be seen that in the cooling process, the external moisture of the soil body crystallizes, indicating that in the slow freezing process, the cold air of the test chamber will firstly contact with the upper surface of the matched soil sample, and the cold air will be transmitted from the top to the bottom, and after that, it will cause the moisture of the surrounding area to gather to the low temperature, and the moisture will appear to be migrated from the internal to the external process. It can be predicted that in the freezing process, the aggregated ice will continuously affect the friction between the geocell and the soil body.

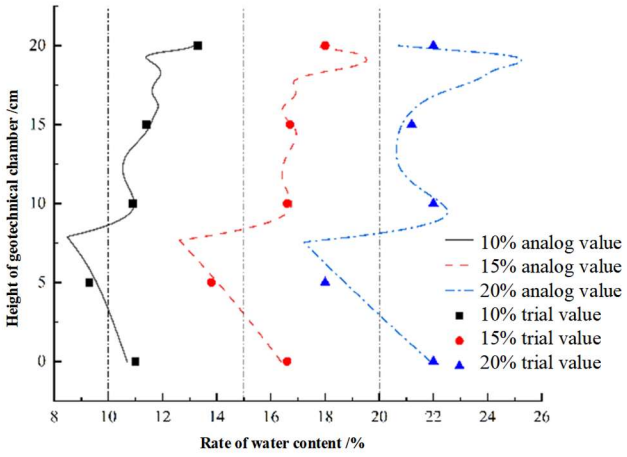

(a) Ice crystals on the surface of frost heave soil samples (b) Water content variation of frost heave test (120h)

Figure 7: Variation of water content in frozen and swollen soil samples (120h)

Fig. 7(b) shows the change of water content at different depths after 120h freezing of soil samples in geogrid chamber with different water content, comparing the results of water content, the numerical simulation results are basically in line with the experimental results, it can be seen from the height of the top position in the figure, in the process of freezing, freezing of the soil body starts to occur from the top down, the freezing front is constantly moving downward, and the water content in the freezing region is higher than the initial water content, this is due to the fact that at the low temperature where the un liquid water in the unfrozen zone undergoes a phase change into ice, while moisture migrates towards the freezing front [16]. While at the bottom position of geocell soil samples water content shows a monotonically decreasing trend, this is because sandy soils have a weaker water-holding capacity compared to clay soils, and at the same time the bottom is less affected by the temperature and more significantly by the gravitational potential, which is the same as the literature [18] in a freezing process of water infiltration from the top to the bottom and with the rise in the water content, the free water content of soils increases, and the migration of liquid water at the bottom increases. In addition, it can be seen that there is a large difference between the experimental and simulated values of water content at the top, which is due to the fact that the top of the experimental soil freezes into ice aggregates, which results in an increase in water content in the top region of the soil sample.

IV. C. Effect of water content on deformation of geocells

IV. C. 1) Analysis of strain field changes

The strain changes at the centerline of the geocell wall and at the welded seam of the cell are given in Figures 8 and 9, respectively. From the figures, it can be seen that under the same water content, the strains in different parts of the geocell are different and have a nonlinear distribution. At different heights, the strain of geocell specimens varied greatly under different water content changes. With the increase of water content, the maximum strain of the wall of the chamber starts to develop from the top of the chamber to the middle and lower part of the chamber. The analysis shows that the compartment specimen freezes from top to bottom and is stretched by the freezing effect of different water content, resulting in tensile strain in the compartment wall, and when the water content exceeds a certain amount, the strain in the geocell specimen starts to change from large to small from top to bottom, which is due to the fact that in the process of deformation, the shape of the geocell starts to optimize from the initial ellipse to a circle, which serves as a role of stress diffusion [19].

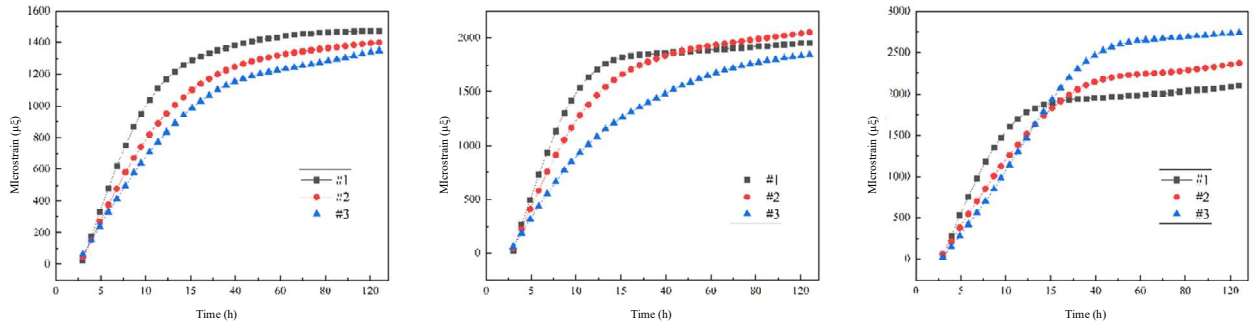

Figure 8: Strain variation of the centerline of geocell wall

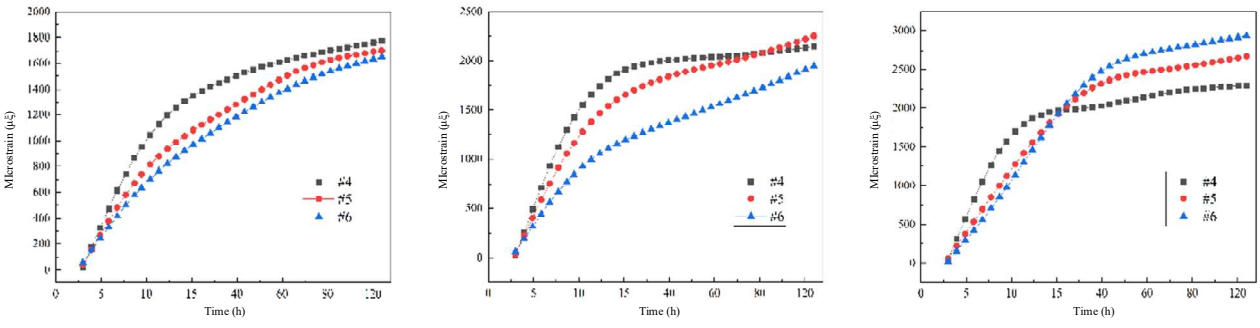

Figure 9: Variation of strain in geogrid weld

IV. C. 2) Displacement field variation analysis

Figure 10 shows the freezing displacement of geocell specimen under different water content in the freezing process, and the analysis shows that the freezing deformation of the soil body develops faster before freezing for 30h, which is due to the fast temperature transfer rate at the cold end, and the upper pore space is filled by the ice rapidly, and then freezing expansion occurs. In the later stage of freezing, the freezing deformation is slower, and the final amount of freezing expansion is 0.76mm, 0.88mm, 1.02mm.Meanwhile, the higher water content has obvious deformation effects on the geocell specimens. Comparing the simulated values of 15% water content, it was found that the trend of the frozen expansion amount was similar to that shown in the results of the test values.

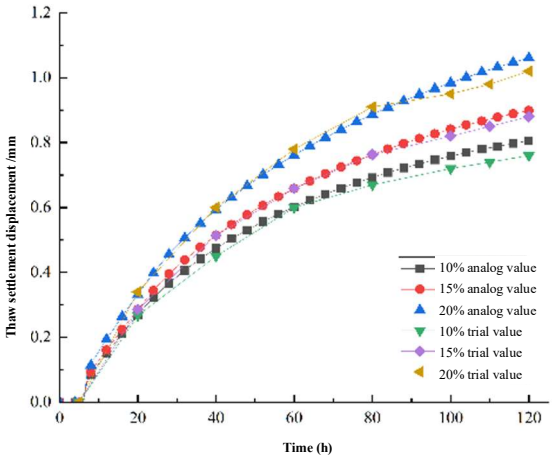

Figure 10: Frost heave displacement at different water contents

IV. D. Effect of different shapes of geocells on frost deformation

IV. D. 1) Analysis of stress field changes

Fig. 11 shows the three-dimensional stress cloud diagrams of different shapes of cells after 120h freeze-up test. From the figure, it can be seen that after 120h freezing and expansion process, different shapes of cells are bearing larger stress at the weld joints, while the contact stress of the middle cell sheet is smaller, indicating that when the geocell is subjected to the freezing and expansion force of the soil and lateral expansion occurs, it is also the nodes that are subjected to larger stresses and lead to damage [19]; the contact stress between the cell and the soil body along the direction of the height of the geocell presents a tendency of large at the top and small at the bottom, the top of the cell has the largest contact stress, and the contact stress at the bottom is smallest. The contact stress at the top of the chamber is the largest, and the contact stress at the bottom is the smallest, which is due to the fact that when the temperature penetrates downward, the soil samples start freezing from the top, and the filler expands when subjected to the freezing and expansion force, and the chamber itself is tensile but not compressive, which results in the filler freezing and expanding in the horizontal direction will be restricted. By comparing the maximum contact stress of geocells of different shapes, it is found that there are square=20kPa>ellipse=16kPa>circle=14kPa, which shows that among all shapes, the circular cell has the best performance in terms of stress under loading.

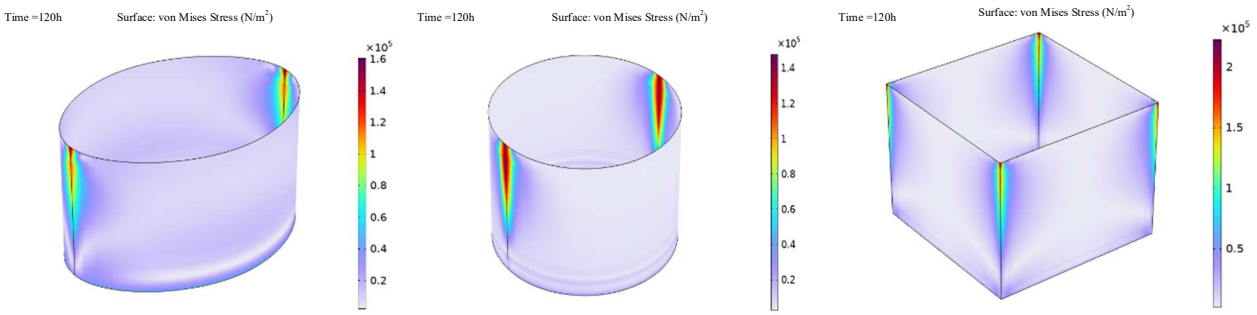

Figure 11: Distribution cloud of contact stress between different shaped cells and packing material (120h)

IV. D. 2) Displacement field variation analysis

Take different shapes of geocells with height of 0.02m and the center is 1/2 radian (1/4 radian of square cell) of the center line of the cell wall as the displacement monitoring, the monitoring results are shown in Fig. 12.

As can be seen from the figure, three different geocells, all in the chamber at the center line of the largest displacement deformation, square, oval, circular maximum horizontal displacement of 0.58mm, 0.94mm, 0.43mm, respectively, different shapes of the chamber in the freezing and expansion of the force under the action of the deformation of the force is not uniformly distributed along the entire length of the chamber, and then in order to the two sides of the decreasing [20], the freezing and expansion of the chamber in the center of the deformation of the largest, but the force is small, indicating that The stress at this place is released with the movement of geocell and soil. In the deformation of different chamber shapes, the horizontal displacement range produced by the circular constrained soil is the smallest, followed by square, and the horizontal displacement produced by the soil constrained by the elliptical geocell is the largest, which can be seen that the difference in the freezing and expansion force applied to the geocells leads to a slight difference in the size of the displacements, and the different shapes of chambers are subjected to different forces, which leads to a large difference in the size of the displacements.

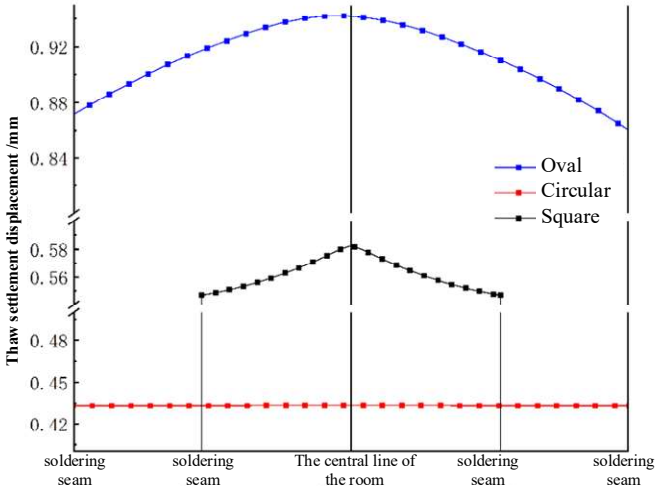

Figure 12: Geocell frost heave displacement (0.02m)

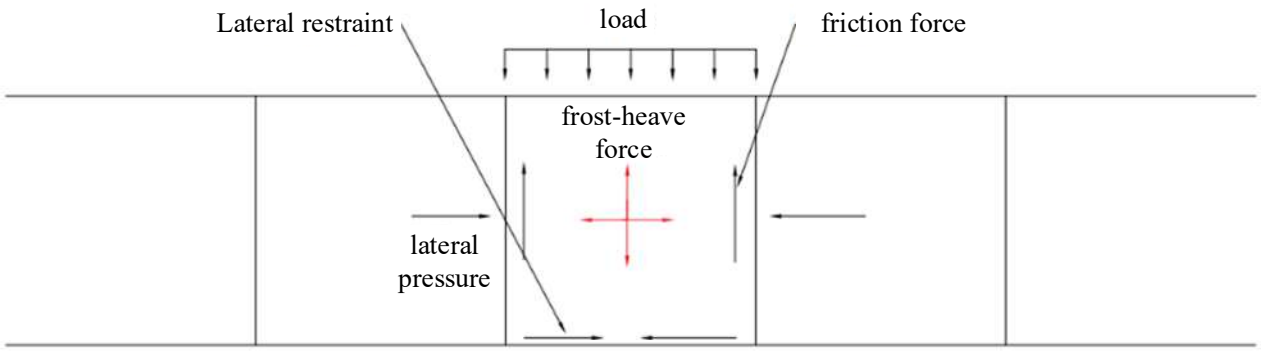

Figure 13: Schematic diagram of geocell stress

IV. E. Analysis of geocells to inhibit frost heave

Literature found that the existing domestic and international geocell reinforced soil reinforcement mechanism [21], are the restraining effect of geocell on soil body under the action of upper load. And from Fig. 13 and the test, it can be seen that when the geocell is reinforced in the permafrost zone, in addition to the upper load, friction, lateral pressure and lateral restraining force, it is also subjected to the active role of the freezing and expansion force in the soil, and the soil freezes and expands in the interior of the geocell, which is limited horizontally by the lateral

restraining effect of the geocell, and vertically by the loading and friction; the effect of the freezing and expansion force of the soil inside the compartments is the effect on the The effect of soil freezing and expansion inside the geocell is the pressure on the surrounding geocell, so the lateral pressure on the geocell should include the soil freezing and expansion.

V. Conclusion

In this chapter, low-temperature freezing and expansion tests are carried out on individual geocell-reinforced sandy soil specimens with different moisture contents. By analyzing the data obtained from the freezing process of the soil body and geocell structure under low-temperature conditions, we obtain the temperature, moisture, displacement and freezing and expansion strain patterns of the contact surface of the geocell-soil in the process of soil freezing; on the basis of the tests, we introduce the model of the freezing and expansion of a single geocell and further analyze the effects of different cell shapes and types on the effectiveness of geocell reinforcement under changes in temperature and moisture. The modeling and simulation of different shapes of compartment cells were carried out respectively, and the influence of different compartment cell shapes on the reinforcing effect of geocells under the changes of temperature and moisture was thus analyzed and explored. The conclusions are as follows:

(1) Based on the freezing and expansion test of a single geocell, a three-dimensional numerical model of reinforced sandy soil with a single geocell was established, and by comparing and analyzing the changes of temperature, moisture and displacement at the top of the cell at 0.02m, the numerical calculation results compared well with the test data, which verified that the model was accurate and applicable.

(2) During the freezing and expansion process of a single geocell, different parts of the geocell are subjected to different strains, and the strain of the geocell starts from the top to the bottom, and the strain at the welded seam of the geocell is the largest. After freezing and expansion of geocells, the maximum displacement and tension inside the cells exist near the top of the centerline of the cell wall.

(3) Comparing the results of geocell reinforced soil tests with different water contents, it was found that the larger the water content, the larger the strain on the geocells and the larger the freezing displacement. Comparison of the original elliptical, square and circular cell numerical analysis found that for different shapes of cell units, all have different reinforcing effect on the frozen soil and all limit the lateral expansion of the soil, of which the circular cell has the best effect in limiting the freezing expansion of the soil.

(4) By analyzing the reinforcement mechanism of geocells in permafrost zone, it can be seen that under no overburden load, the joint action of ambient temperature and moisture in permafrost zone can make the soil body produce frost heave, and then the geocells are subject to the internal frost heave force and lateral frost heave pressure of the surrounding soil body. In addition, a single geocell in the form of frost deformation process, that is, by the temperature of the top-down transfer of frost deformation, and its deformation is similar to the overburden load.

Funding

This work was supported by the Science and technology projects of Xinjiang transportation industry in 2022 (2022-ZD-005).

References

[1] Liu Jianqi. Construction technology of geocell strengthening subgrade in permafrost wetland[J]. West-China Exploration Engineering, 2005, 17(5): 173-174.

[2] Wang Zhenduo. Study on application of geosynthetics in canal seepage control in frost heave area[J]. China Rural Water and Hydropower, 2006, 48(3): 86-88+91.

[3] Wei Jing, Xu Zhaoyi, Jianjun Jia. Experimental study on embankment slope protection with geocell in premafrost regions of Qinghai-tibet railway[J]. Chinese Journal of Rock Mechanics and Engineering, 2006, 25(z1): 3168-3173.

[4] Wang Tiequan. Study on subgrade and pavement structural deformation characteristics of high-grade highway in permafrost regions[D]. Xi'an: Changan University, 2016.

[5] Wang Liyun. Economic evaluation on rational asphalt pavement in High altitude and cold permafrost area[D]. Xi'an: Changan University, 2017.

[6] Mao Xuesong, Huang Zhe, Zhu Fengjie. Adaptability of pavement typical structure in high altitude cold area[J]. Journal of Chongqing Jiaotong University(Natural Science), 2017, 36(8): 23-29.

[7] Dehghanİan Kaveh, Önder Rukiye. Geocell malzemesinin Özellikleri ve İnşaat sektöründe kullanımı[J]. İleri Mühendislik Çalışmaları ve Teknolojileri Dergisi, 2021, 2(2): 63-74.

[8] Pokharel Sk, Martin I, Norouzi M, et al. Validation of geocell design for unpaved roads[C]// Proceedings of Geosynthetics 2015. Portland, Oregon: Geosynthetics, 2015: 711-719.

[9] Pokharel Sanat, Norouzi M, Breault M. New advances in novel polymeric alloy geocell-reinforced base course for paved roads[C]// TAC 2017: Investing in Transportation: Building Canada's Economy--2017 Conference and Exhibition of the Transportation Association of Canada. 2017.

[10] Pokharel Sanat, Eng Ph Dp, Timothy Yii Eit, et al. High strength geocell and geogrid hybrid reinforcement for compressor station gravel pad on very soft subgrade[C]// Geosynthetics Conference. 2019: 851-859.
[11] Huang Mian, Lin Cheng, Pokharel Sanat K, et al. Model tests of freeze-thaw behavior of geocell-reinforced soils[J]. Geotextiles and Geomembranes, 2021, 49(3): 669-687.
[12] Huang Mian, Lin Cheng, Pokharel Sanat K. Freeze–thaw effects on mechanical behavior of geocell-reinforced sands from element and model tests[J]. International Journal of Geosynthetics and Ground Engineering, 2021, 7(2): 1-13.
[13] Huang Mian, Lin Cheng, Pokharel Sanat K. Evaluation of freeze-thaw behavior of geosynthetics- reinforced base courses[C]// 75th Canadian Geotechnical Conference. Calgary, Alberta: GeoCalgary 2022, 2022: 190-197.
[14] Bai Q B. Determination of boundary layer parameters and a preliminary research on hydrothermal stability of subgrade in cold region[D]. Beijing: Beijing Jiaotong University, 2015.
[15] Tai Bo Wen, Liu Jian Kun, Wang Teng Fei, et al. Numerical modelling of anti-frost heave measures of high-speed railway subgrade in cold regions[J]. Cold Regions Science and Technology, 2017, 39(9): 28-35.
[16] Wei Daokai, Jing Hao, Chen Qi, et al. One--dimensional hydro--thermal--mechanical coupling model and numerical analysis of soils in cold region[J]. Jouranl of Natural Disasters, 2022, 31(5): 150-157.
[17] Yin Changjun, Shu Liang, Pan Ting, et al. Design and application of geocell material based on asymptotic homogenization method[J]. Journal of Railway Science and Engineering 2019, 16(4): 900-906.
[18] Zhang Jianxun, Mao Xuesong, Liu Feifei, et al. Study on water migration behavior of unsaturated soil under unidirectional freezing condition[J]. Journal of Glaciology and Geocryology, 2023, 45(3): 1080-1091.
[19] Hou Juan, Zhang Mengxi, Han Xiao, et al. Mechanism of a high-strength geocell using FEM[J]. Chinese Journal of Geotechnical Engineering, 2015, 37(S1): 26-30.
[20] Han Xiao, Zhang Mengxi, Zhang Jiayang, et al. Deformation analysis of model test of sand foundation reinforced with high-strength geocell[J]. Journal of Shanghai University (Natural Science), 2014, 31(3): 27-33.
[21] Han Jie, Yang Xiaoming, Leshchinsky Dov, et al. Behavior of geocell-reinforced sand under a vertical load[J]. Transportation Research Record, 2008, 2045(1): 95-101.